

Supplementary Information

Antarctic sea-ice loss shifts the Pacific Decadal Oscillation toward its positive phase

**Hyein Jeong^{1,2}, Hyo-Seok Park^{1,2*}, Sang-Wook Yeh^{1,2}, Eui-Seok Chung³, and
Shang-Ping Xie⁴**

¹*Institute of Ocean and Atmospheric Science (IOAS), Hanyang University, Ansan, South Korea*

²*Department of Marine Science and Convergence Engineering, Hanyang University, Ansan, South Korea*

³Division of Ocean and Atmosphere Sciences, Korea Polar Research Institute, Incheon, South Korea

⁴Scripps Institution of Oceanography, University of California San Diego, La Jolla, CA, USA

19 **Contents:**

20

21 **1. Supplementary Tables 1-2**

22 **2. Supplementary Figures 1-6**

23

24 **Supplementary Table 1. | Summary of CESM2 and CM2.1 control (Ctrl) and reduced**
 25 **Antarctic sea ice albedo (rALB) experiments.**

26

Model	Experiment	Ensemble members	Integration length	Antarctic sea ice albedo change (Antarctic only; Arctic unchanged)	Initial conditions
CESM2	Ctrl	5	100 years	None	Restart files from NCAR pre-industrial control
CESM2	rALB	5	100 years	~25% reduction	Same as Ctrl
CM2.1	Ctrl	5	100 years	None	Restart files from GFDL long pre- industrial control
CM2.1	rALB	5	100 years	Stronger reduction; 40% (members 1-3), 60% (members 4-5)	Same as Ctrl

27

28 **Supplementary Table 2. | Summary of CESM2 Asian jet nudging experiments.**

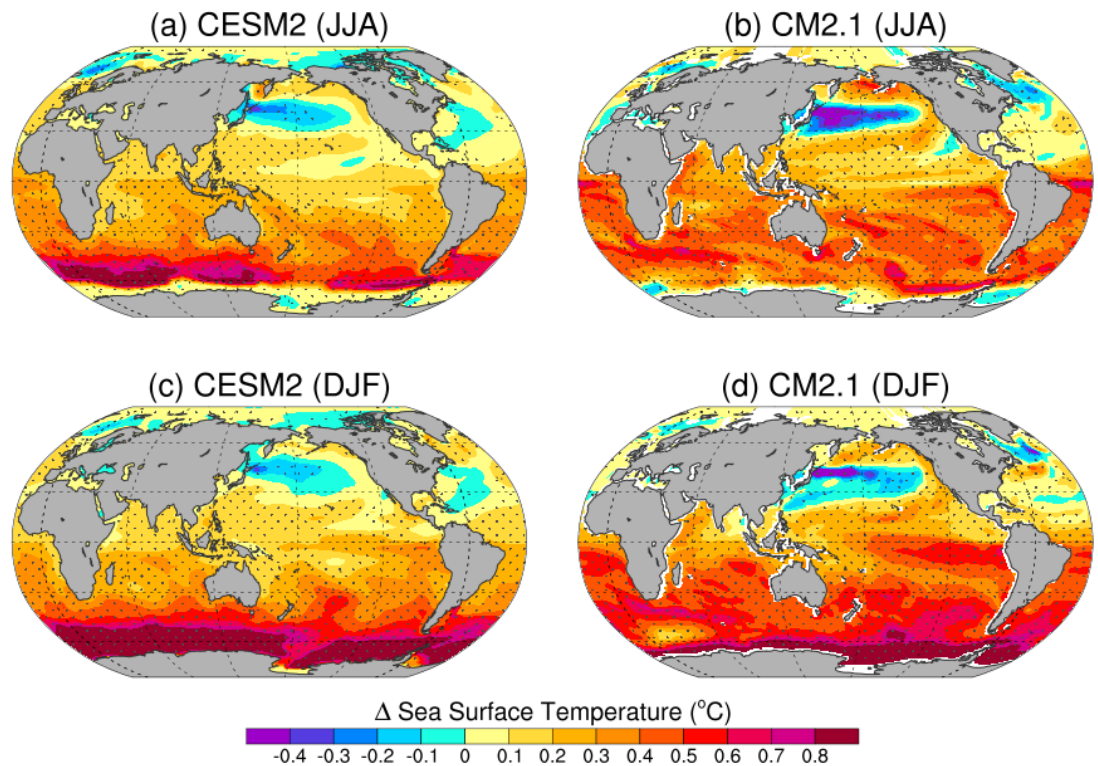
29

Experiment	Target	Ensemble	Integration	Nudging region	Initial
set	climatology	members	length		conditions
for nudging					
Ctrl-nudge	1-30 year monthly climatology from CESM2	3	30 years	28°–53°N, 40°– 90°E (Tibetan Plateau, see green box in Fig. 3a)	Restart files from NCAR pre-industrial control
rALB-nudge	1-30 year monthly climatology from CESM2	3	30 years	Same as above	Same as Ctrl
	rALB				

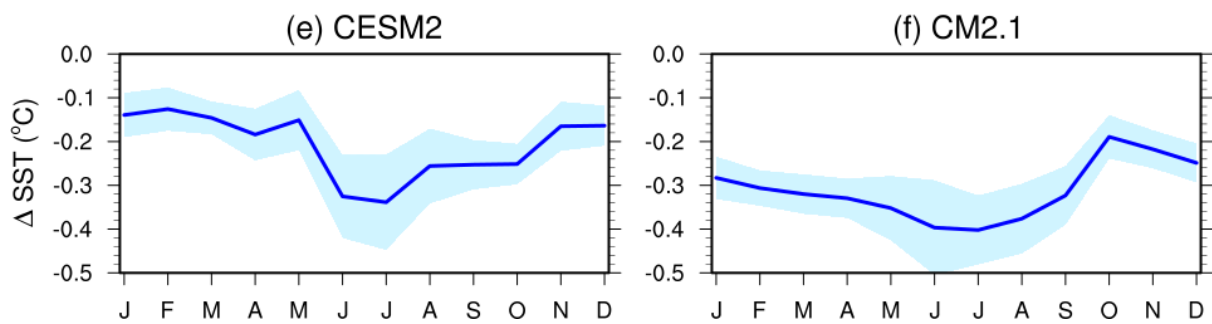
30

31

Transient SST responses to Antarctic sea ice loss during JJA and DJF



Seasonal cycle of Northwestern Pacific SST anomalies

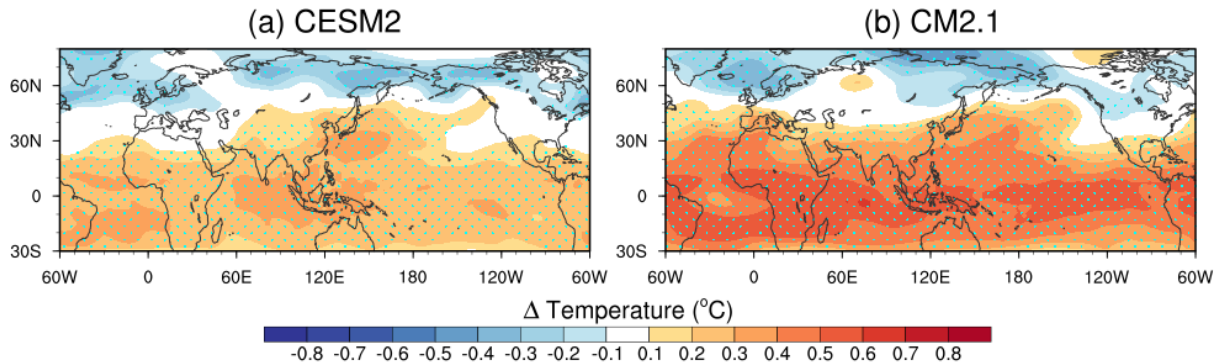


32

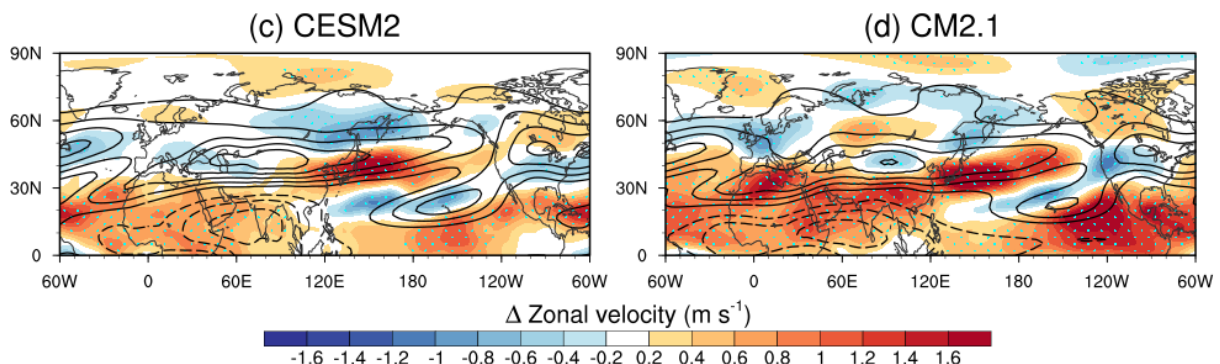
33 **Supplementary Fig. 1 | Seasonal SST responses to Antarctic sea ice loss in CESM2 and**
 34 **CM2.1 models.**

35 **(a, b)** Sea surface temperature (SST; °C) anomalies averaged over years 1–20 in **(a)** CESM2
 36 and **(b)** CM2.1 during June–July–August (JJA). Stippling indicates regions where anomalies
 37 are statistically significant at the 95% confidence level. **(c, d)** Same as (a, b), but for December–
 38 January–February (DJF). **(e, f)** Seasonal cycle of SST anomalies (°C) in the northwestern
 39 Pacific (30°–60°N, 120°E–160°W), with the solid line denoting the ensemble mean and shading
 40 indicating the inter-member spread (± 1 standard deviation).

Δ Temperature at 200-hPa



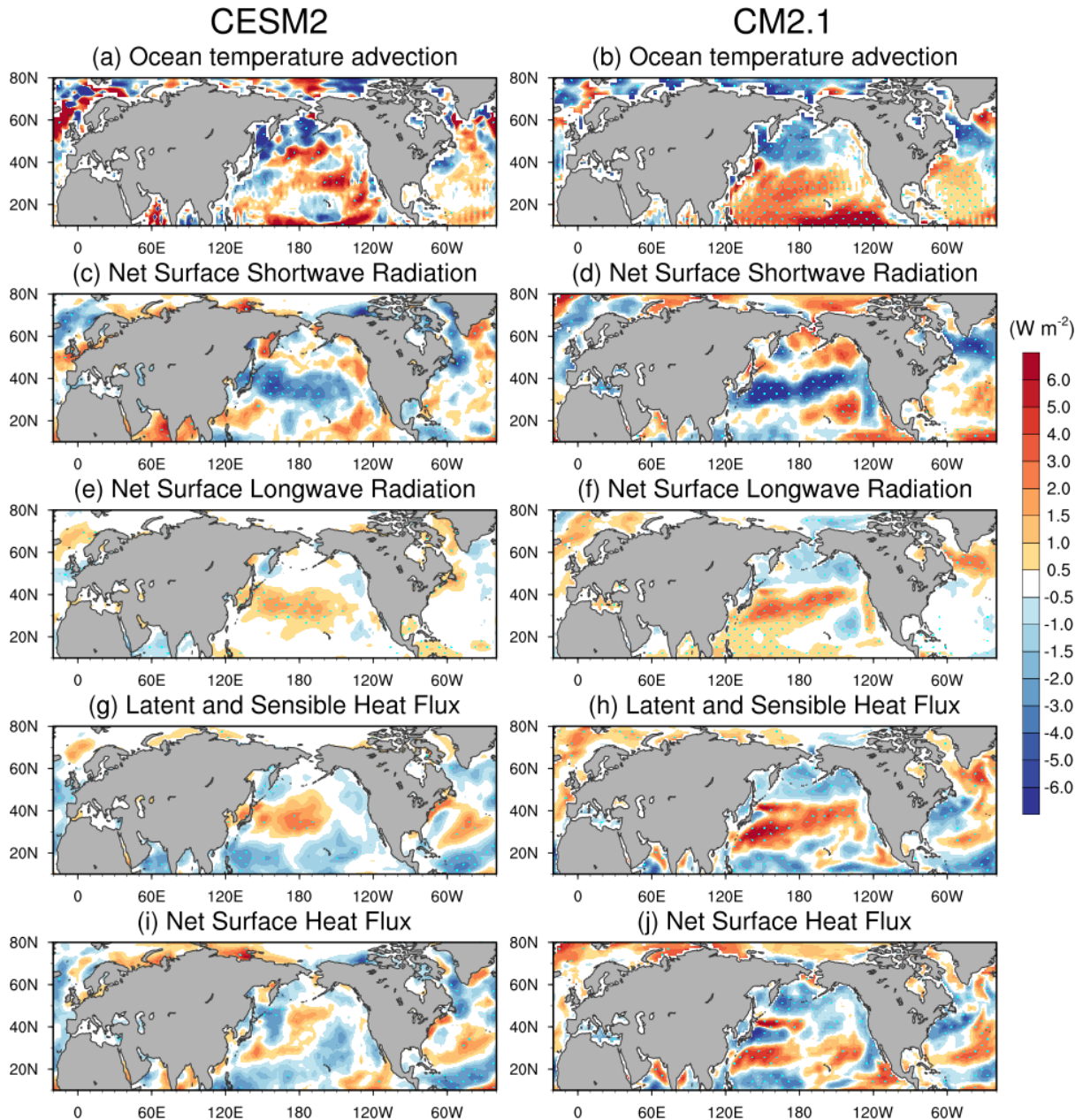
Δ Zonal velocity at 200-hPa



41

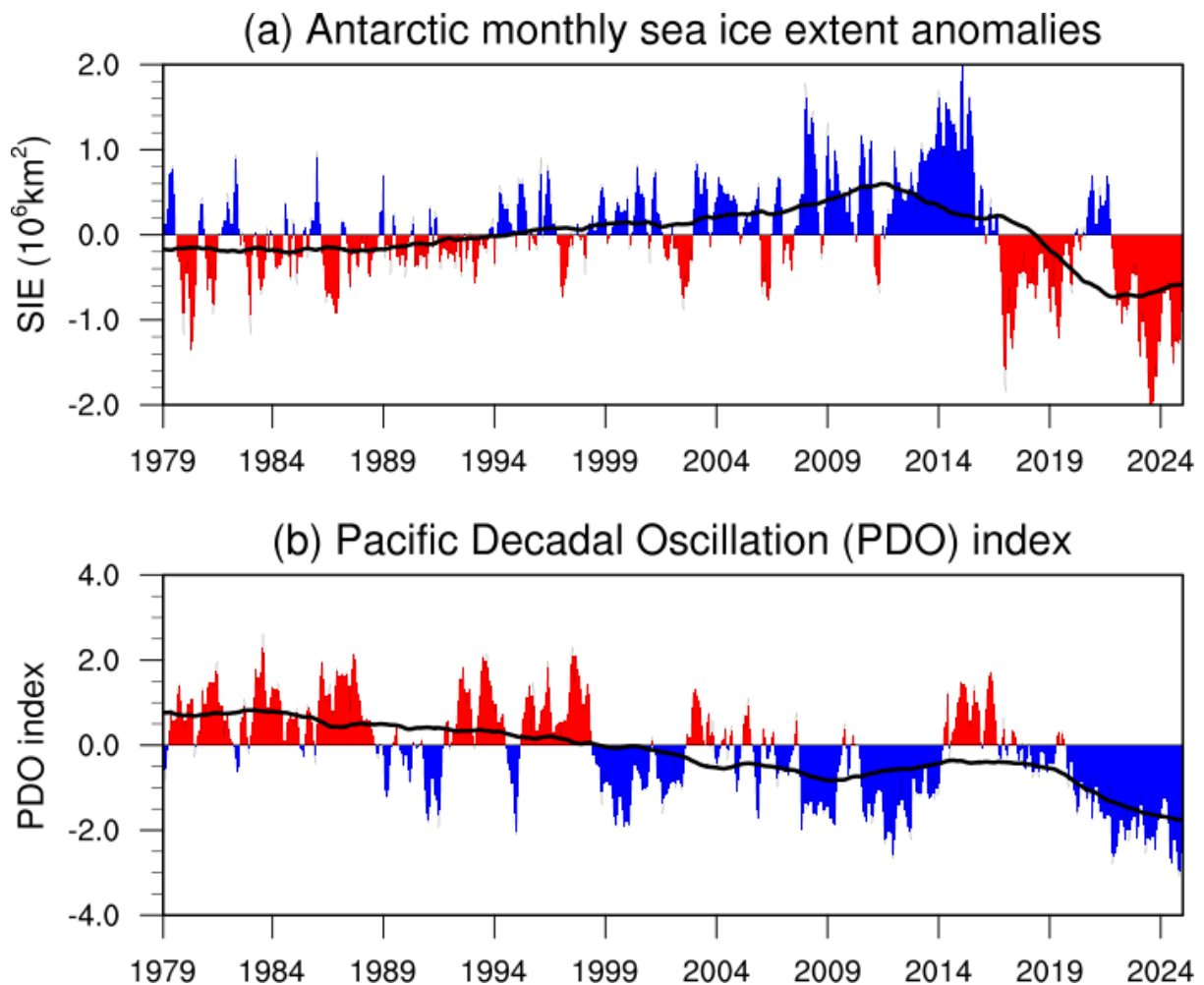
42 **Supplementary Fig. 2 | Atmospheric response to Antarctic sea ice loss in CESM2 and**
 43 **CM2.1 models.**

44 **(a, b)** Temperature anomalies ($^{\circ}\text{C}$, shading) at 200 hPa in June–July–August (JJA) due to
 45 reduced Antarctic sea ice albedo for (a) CESM2 and (b) CM2.1, averaged over years 1–30 of
 46 the 100-year integration to represent the transient response. **(c, d)** Same as (a, b), but for zonal
 47 wind anomalies (m s^{-1} , shading). Contours in (c, d) show the climatological zonal wind (m s^{-1}).
 48 Statistically significant values ($p < 0.05$) are stippled.



Supplementary Fig. 3 | Surface energy budget responses to Antarctic sea ice loss in CESM2 and CM2.1 models.

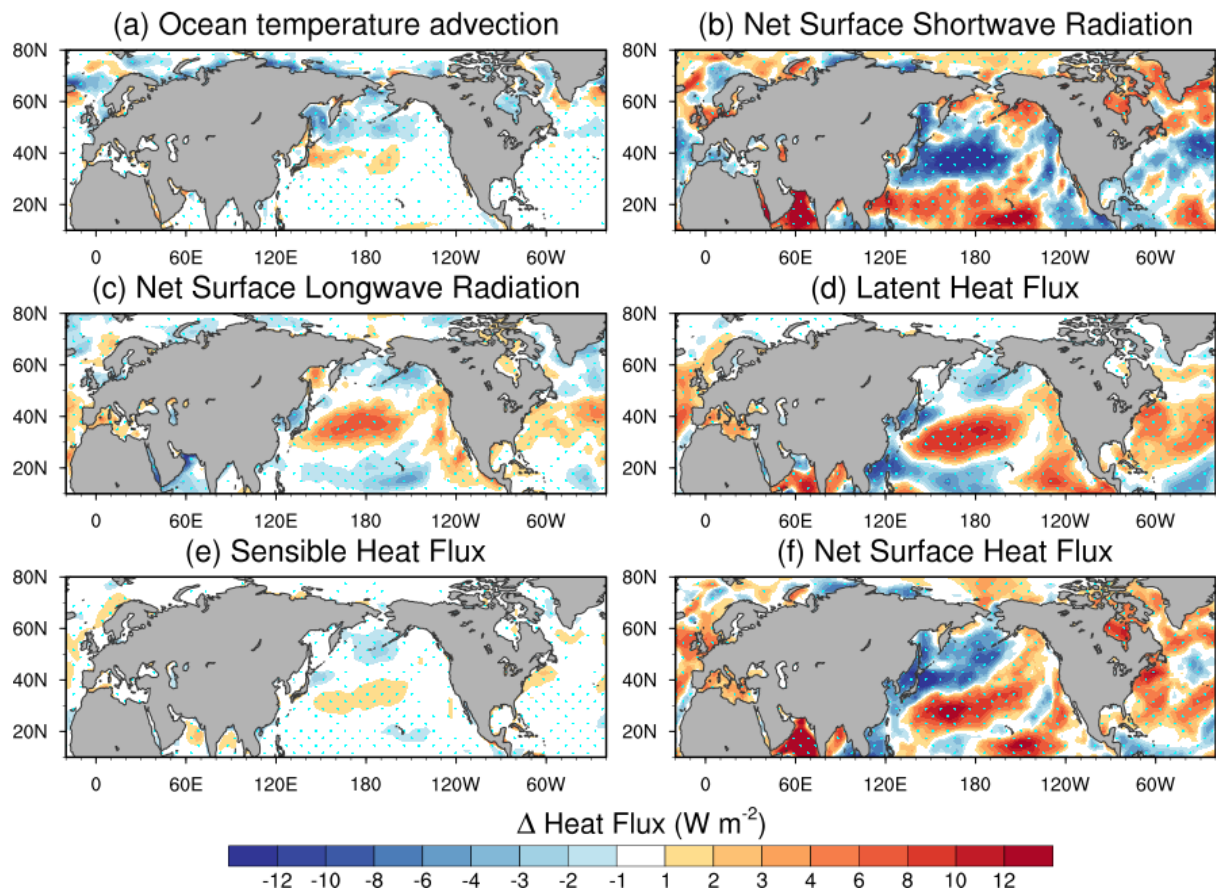
52 **(a, b)** Ocean temperature advection anomalies for (a) CESM2 and (b) CM2.1. The advection
 53 term is originally diagnosed in units of K s^{-1} and converted into an equivalent surface heat flux
 54 (W m^{-2}) by multiplying with seawater density, specific heat capacity, and local mixed layer
 55 depth. **(c, d)** Same as (a, b), but for net surface shortwave radiation anomalies (W m^{-2}). **(e, f)**
 56 Same as (a, b), but for net surface longwave radiation anomalies. **(g, h)** Same as (a, b), but for
 57 latent and sensible heat flux anomalies. **(i, j)** Same as (a, b), but for net surface heat flux
 58 anomalies. All anomalies are averaged over years 1–30 of the 100-year integration to represent
 59 the transient response. Statistically significant values ($p < 0.05$) are stippled.



61 **Supplementary Fig. 4 | Observed Antarctic sea ice extent anomalies and Pacific Decadal
62 Oscillation (PDO) index.**

63 **(a)** Monthly Antarctic sea ice extent (SIE) anomalies (10^6 km 2) relative to the 1979–2024
64 climatology. Blue (red) bars indicate positive (negative) anomalies. **(b)** Monthly PDO index
65 for 1979–2024. Red (blue) bars indicate positive (negative) phase of PDO. In both panels, the
66 black line denotes the 10year running mean.
67

Idealized experiment of Asian jet southward



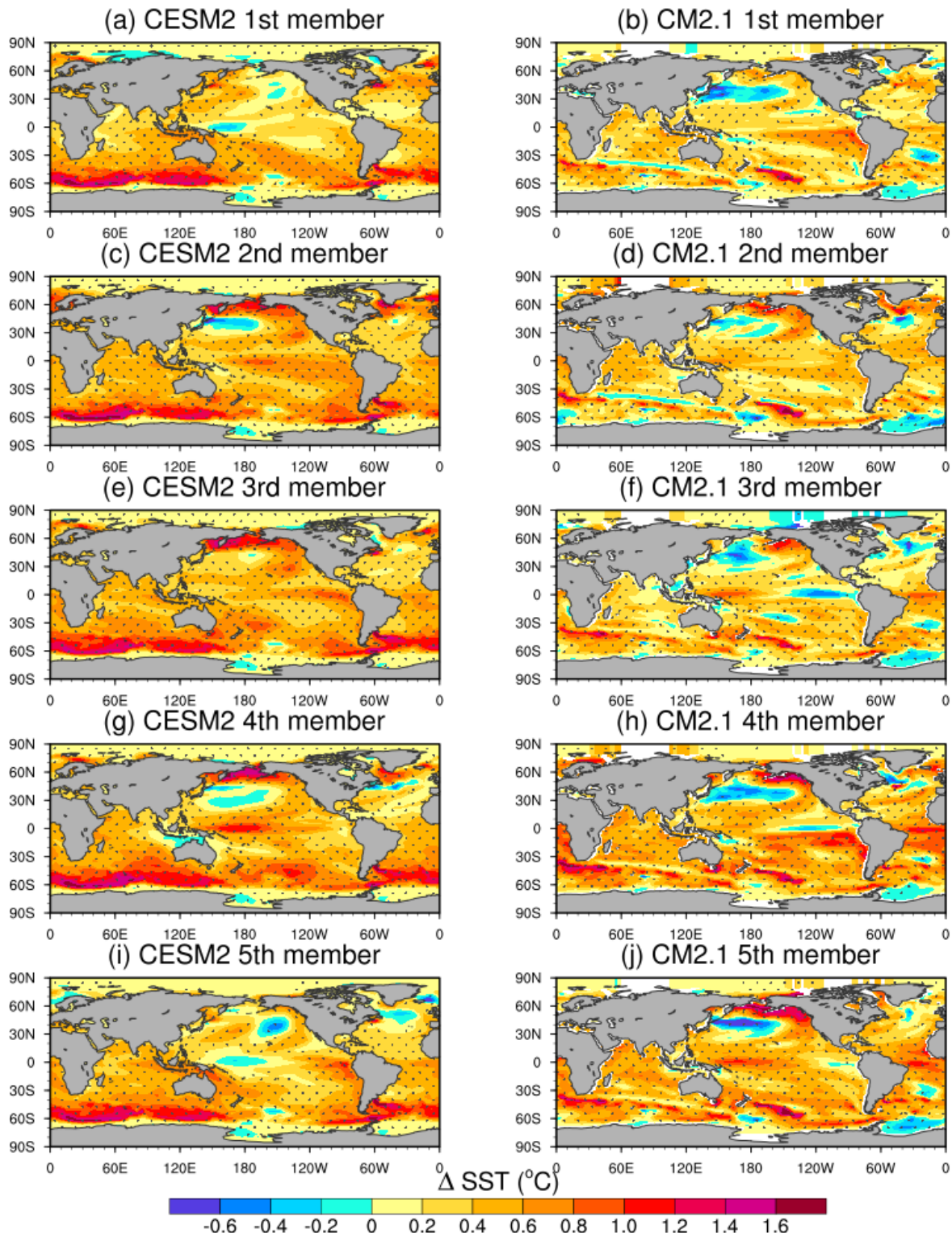
68

69 **Supplementary Fig. 5 | Surface energy budget anomalies from the idealized experiment**
70 **of the southward shift of the Asian jet.**

71 **(a)** Ocean temperature advection anomalies, originally diagnosed in K s^{-1} and converted to W m^{-2} by multiplying with seawater density, specific heat, and local mixed layer depth. **(b)** Net surface shortwave radiation (W m^{-2}), **(c)** Net surface longwave radiation, **(d)** Latent heat flux, **(e)** Sensible heat flux, and **(f)** Net surface heat flux anomalies. All anomalies are shown for June–July–August (JJA). Stippling indicates statistically significant values ($p < 0.05$).

76

SST responses to Antarctic sea ice loss (71-100 years)



77

78

79 **Supplementary Fig. 6 | Global SST responses to Antarctic sea ice loss in CESM2 and**
 80 **CM2.1.**

81 (a–j) June–July–August (JJA) mean SST anomalies ($^{\circ}\text{C}$, shading) averaged over years 71–100
82 of the 100-year integration, representing the quasi-equilibrium response to reduced Antarctic
83 sea ice albedo. Results are shown for five ensemble members from CESM2 (a, c, e, g, i) and
84 CM2.1 (b, d, f, h, j). Stippling denotes statistically significant values ($p < 0.05$).

85